Hydrogenic Spectroscopy

Edward Jin
MIT Department of Physics
(Dated: March 18, 2022)

First, by measuring the atomic emission lines of hydrogen, the Rydberg constant of hydrogen was measured to be $R_H = (1.096764 \pm 0.000013_{stat} \pm 0.000070_{sys}) \cdot 10^7 \mathrm{m}^{-1}$, in close agreement with the accepted value of $1.096776 \cdot 10^7 \mathrm{m}^{-1}$. Second, by measuring the shift of the atomic emission lines between hydrogen and deuterium, the Hydrogen-Deuterium mass ratio was determined to be $0.495 \pm 0.012_{stat}$, in agreement with the accepted value of 0.500. Finally, various lines of the sodium spectrum were measured, and the energy splitting between the $J = 3/2$ and $J = 1/2$ state of the $3p$ orbital was measured to be $(2.155 \pm 0.010)\,\mathrm{meV}$, in agreement with the accepted value of $2.15\,\mathrm{meV}$. Comparing the splitting of the $4p$ and $3p$ orbitals, the ratio of splitting energies was found to be similar to $\frac{4^3}{3^3}$, as predicted by the semi-empirical rule.

I. INTRODUCTION

In the early 1900s, the optical spectrum of hydrogen was measured and the lines themselves were found to follow the Balmer formula, a simple formula predicting the wavelengths of emission as $\frac{1}{\lambda} = R_H \left(\frac{1}{4} - \frac{1}{n^2} \right)$, where R_H is the Rydberg constant for Hydrogen. The simplicity of the formula led Bohr to develop the idea of quantization of atomic energy levels, which was able to explain these spectra. While Bohr's formula utterly fails at atoms with higher atomic number, it can explain the spectra of hydrogenic atoms quite well.

If the spectrum of deuterium is measured, we would expect nearly the same emission spectra, as hydrogen and deuterium only differ by a neutron. However, the reduced mass of the deuterium system is slightly higher, due to the increase in nucleus mass. This causes the Rydberg constant of deuterium to be higher by a factor of $\frac{\mu_D}{\mu_H}$, where μ_D and μ_H are the respective reduced masses of hydrogen and deuterium. This difference manifests in a small shift in the emission lines of deuterium, which allows for calculation of the H-D mass ratio.

Further developments to quantum theory by Dirac and others led to corrections to the energy levels of hydrogenic atoms, by taking relativistic effects and spin-orbit coupling into account. This effect is hard to see in hydrogen itself, as the splitting is about 0.08 Angstroms. However, the splitting scales with the fourth power of atomic number, meaning that this effect is much more pronounced in Sodium [1].

Sodium can be modeled as approximately hydrogenic, as we can assume that only the 3s-electron ionizes, while the inner electrons from lower-lying orbitals do not ionize. The additional inner electrons can instead be interpreted as a perturbation of a hydrogenic system. The splitting leads to measurable differences in the emission spectra, resulting from atomic transitions to different spin states.

In this experiment, we measure the atomic emission spectra of hydrogen, deuterium, and sodium, in order to verify the Balmer formula, measure the mass ratio between the proton and the deuteron, and examine the fine structure of sodium.

FIG. 1. A monochromator similar to the one used in the experiment. The entrance and exit slits are on the left face.

II. EXPERIMENTAL SETUP

A Jobin Yvon 1250M monochromator was used to measure the emission spectra of various atoms. The monochromator focuses light from the emission source to make a beam that is directed towards a 1800 lpmm diffraction grating, effectively filtering the input light to one wavelength. The photons then hit a photomultiplier tube (set at 900 V DC), which counts the number of incident photons per second at that wavelength and converts the counts to an electrical signal that can be analyzed on a desktop computer.

The diffraction grating was moved in 0.01 Å increments for all measurements, unless noted otherwise. The recorded peak wavelength was that at which the maximal photon count rate was measured. Integration times and slit widths were chosen to sufficiently resolve peaks; for high-intensity peaks, 10 µm slit widths with 100 ms were sufficient, while 100 µm slit widths and integration times ranging from 500 to 2000 ms were needed for low-intensity peaks.

III. EXPERIMENTAL PROCEDURE

III.1. Mercury/Krypton Calibration

First, the emission spectrum of mercury was measured over 11 wavelengths from 3125.67 Å to 5790.66 Å. The emission spectrum of Krypton at 7587.41 Å and 7601.55
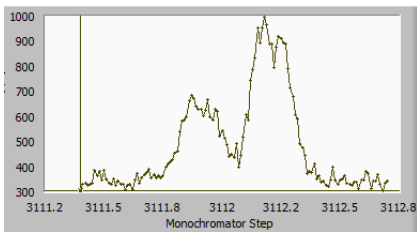
FIG. 2. A mercury doublet. Though the peaks are separated only by 0.3 Å, the spectrometer can clearly differentiate them from each other and the background.

Å was also measured to obtain higher-wavelength measurements for calibration. The values obtained were compared to the ones listed in the NIST database [2], and were used to calibrate the monochromator for interpolation. As the measurements of the monochromator varies day-to-day, the spectra of mercury and krypton were remeasured every day and were used to calibrate solely that day's measurements.

III.2. Hydrogenic Measurements

Interestingly, the deuterium tube contained approximately 40% hydrogen, and so the deuterium tube was used for measurements of the spectrum of both hydrogen and deuterium. The emission spectra wavelengths were measured in triplicate near the expected Balmer wavelengths that correspond to the transitions between $n = 3, \ldots, 7$ states to the $n = 2$ state. The exact identity of which peak corresponding to which atom was confirmed by measuring the emission spectrum of pure hydrogen, which was indeed found to have higher-wavelength emission peaks. In addition, the temperature of the room was measured to correct the refractive index.

III.3. Sodium Measurements

The sodium spectrum was first scanned from 3200 Å to 6200 Å in 0.15 Å increments with 100 μm slit widths to obtain a broad spectrum. All peaks in the low-resolution scan above 2000 counts per second were compared to peaks in the NIST database and identified, if possible [2]. All sodium peaks found in the low-resolution scan were then scanned again in 0.01 Å increments and measured in triplicate. Low-intensity peaks were scanned in quintuplicate with higher integration times.

IV. RESULTS AND ANALYSIS

IV.1. Calibration

First, the peak data for Mercury/Krypton differed by up to 0.06 Å over three runs, and had a maximum de-
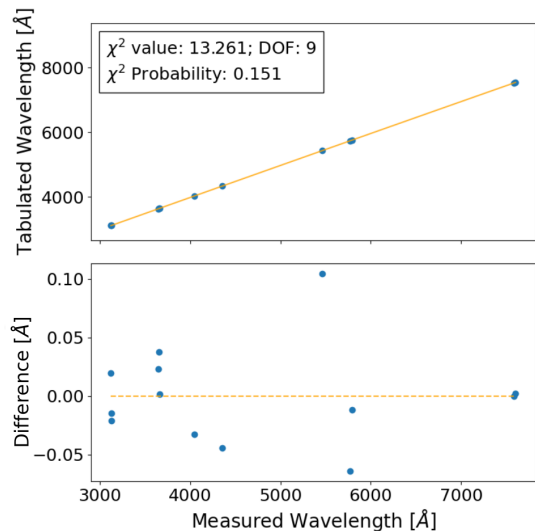

FIG. 3. The cubic fit to the calibration data, and the differences between the fit and actual value. The fit itself looks reasonable and the maximum difference is around 0.1 Å.

viation from the mean of about 0.03 Å. There is also an additional uncertainty of 0.01 Å as the monochromator only has 0.01 Å resolution. Thus, the uncertainty of each measured wavelength from instrumentation was estimated to be 0.04 Å.

In order to calibrate the monochromator, we performed polynomial fits from the measured Mercury/Krypton average emission peaks to the tabulated NIST peaks. Linear and quadratic fits yielded a chi-square value over 100 and a corresponding probability of 0.0%, with maximum difference above 0.2 Å. A cubic fit performed much better and yielded a chi-square value of about 10 with a corresponding probability of about 15%, and had maximum difference of about 0.1 Å. A quartic fit performed similarly to the cubic fit. As the cubic fit was sufficient, it was used for all conversions between measured peak wavelength and actual peak wavelength, and any peaks reported in this paper are corrected-wavelength ones.

To determine the uncertainty of the calibration procedure, we attempted to measure the quality of interpolation. To do so, we first removed any data points that were within 10 Å of each other, in order to make sure that all the data points were not strongly correlated with each other. Then, we excluded a singular point from the dataset, performed the cubic fit, and recorded the deviation of the cubic fit of the excluded point. This was done for every non-endpoint point in the data, and the maximum deviation was taken to be the uncertainty of the fit, which was 0.11 Å. Combining the uncertainties from instrumental resolution, instrumental accuracy, and calibration accuracy, we report each wavelength measurement with 0.12 Å uncertainty by default. This uncertainty is also quite similar to the maximum deviation of the cubic fit from the data itself.

IV.2. Determination of the Rydberg Constant

The Rydberg constant for hydrogen can be determined with the Balmer formula, as

$$R_H = \left(\lambda \cdot \left(\frac{1}{4} - \frac{1}{n^2} \right) \right)^{-1}$$

where λ is the wavelength in vacuum and n is the initial energy level of the atom. As our measurements of λ were in air, we multiply our original measurements by the refractive index of air, to obtain the corresponding wavelength in vacuum. Over the wavelengths of interest at the room temperature of 24 C, the refractive index of air is 1.000265 ± 0.000001 [3][4]. Given the uncertainty of the refractive index and of the wavelength measurements, we calculate the following measurements of the Rydberg Constant of Hydrogen:

Transition	Wavelength (Å)	Rydberg Constant (m^{-1})
$n = 3 \to 2$	6562.99 ± 0.12	$(1.096770 \pm 0.000020) \cdot 10^7$
$n = 4 \to 2$	4861.27 ± 0.12	$(1.096817 \pm 0.000027) \cdot 10^7$
$n = 5 \to 2$	4340.55 ± 0.12	$(1.096783 \pm 0.000030) \cdot 10^7$
$n = 6 \to 2$	4102.00 ± 0.12	$(1.096736 \pm 0.000032) \cdot 10^7$
$n = 7 \to 2$	3970.41 ± 0.12	$(1.096714 \pm 0.000033) \cdot 10^7$

These measurements largely agree with their average within a 2σ bound, and the average Rydberg constant can be calculated from these measurements to be $(1.096764 \pm 0.000013) \cdot 10^7 \text{m}^{-1}$. Finally, there are also systematic uncertainties arising from the fact that the Bohr model is not perfect; the relativistic correction changes the energy of the ground state by $9 \cdot 10^{-4}$ eV [5], corresponding to 700 m^{-1}, and other such corrections are of this order of magnitude. Adding this uncertainty into the measurement, we calculate the value of the Rydberg constant for Hydrogen as

$$R_H = (1.096764 \pm 0.000013_{stat} \pm 0.000070_{sys}) \cdot 10^7 \text{m}^{-1}$$

which is in good agreement with the accepted value of $1.096776 \cdot 10^7 \text{m}^{-1}$.

IV.3. Determination of the H/D mass ratio

The main difference in the emission lines between a hydrogen and a deuterium atom can be explained almost entirely by the change in reduced mass [1]. Applying a few approximations from the reduced mass formula, we have that

$$\frac{m_P}{m_D} = 1 - \frac{m_P}{m_e} \cdot \frac{\Delta\lambda}{\lambda}$$

No other uncertainties were considered as the reduced mass accounts for nearly the entire difference.

Using the tabulated value of $\frac{m_P}{m_e} = 1836.1527$ [6], we can then calculate the deuteron-proton mass ratio. As the calibration uncertainties are likely to be extremely
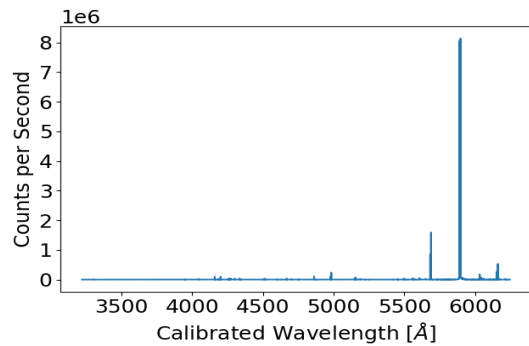

FIG. 4. The results of the rough scan of the sodium spectrum. The spectrum is dominated by the D-line doublet, and the second largest peak is the $4d \to 3p$ transition around 5685 Å. Other peaks are scattered throughout the spectrum, with many in the 5500-6500 Å range.

similar for the Hydrogen and Deuterium measurements, the uncertainty in the wavelength difference is reduced as compared to the general case. Looking at how the cubic fit performs on similar wavelengths, we estimate that the calibration uncertainty for similar wavelengths is around 0.05 Å, rather than 0.11 Å as in the general case. Combining this uncertainty with the 0.04 Å instrumental uncertainty, the total uncertainty in the wavelength shift is 0.06 Å.

Transition	Wavelength Shift (Å)	H-D Mass Ratio
$n = 3 \to 2$	1.82 ± 0.06	0.492 ± 0.018
$n = 4 \to 2$	1.34 ± 0.06	0.493 ± 0.024
$n = 5 \to 2$	1.21 ± 0.06	0.488 ± 0.027
$n = 6 \to 2$	1.13 ± 0.06	0.492 ± 0.029
$n = 7 \to 2$	1.06 ± 0.06	0.509 ± 0.030

These measurements also agree with their average within a 1σ bound, and the average Hydrogen-Deuterium mass ratio can be calculated to be $\frac{m_H}{m_D} = 0.495 \pm 0.012$ which is in good agreement with the accepted value of 0.500.

IV.4. Sodium Atom Measurements

By comparing the peak locations and intensities in the rough scan to the NIST database, Argon and Hydrogen were found to be known contaminants in the lamp. Other unexpected peaks were unable to be identified, but potential candidates for their presence include Vanadium, Potassium, Iron, and Chromium.

When analyzing the rough scan data, all values under 2000 cps were treated as noise and set to 0. Out of the 512 peaks found after removing noise, 120 were from Argon, 23 from Sodium, 3 from Hydrogen, and the rest were unidentified.

Peaks with intensity above 10000 cps were considered to be major peaks. 42 major peaks were found to originate from Argon, 13 from Sodium, and 2 from Hydrogen. Out of the remaining 57 unidentified major peaks,

51 fell within 50 Å of the high-intensity sodium D lines, and are most likely due to noise, as the sodium D line emissions spill over to neighboring wavelengths in an approximately-50 Å window.

The found sodium peaks are tabulated below, along with the quantum transition giving rise to them. The subscript of the orbital is the total angular momentum. When two transitions are close in energy and lead to the same emission wavelength, the angular momenta are separated with a |. This often happens when the transitions are from d-orbitals, as the splitting of the d-orbital levels is much weaker.

λ (Å)	Transition	Doublet Splitting (meV)
3302.37	$4p_{3/2} \to 3s_{1/2}$	0.717 ± 0.074
3303.00	$4p_{1/2} \to 3s_{1/2}$	
4389.99	$8d_{3/2} \to 3p_{1/2}$	2.168 ± 0.042
4393.36	$8d_{3/2|5/2} \to 3p_{3/2}$	
4420.03	$9s_{1/2} \to 3p_{1/2}$	2.132 ± 0.040
4423.39	$9s_{1/2} \to 3p_{3/2}$	
4494.26	$7d_{3/2} \to 3p_{1/2}$	2.130 ± 0.040
4497.73	$7d_{3/2|5/2} \to 3p_{3/2}$	
4541.60	$8s_{1/2} \to 3p_{1/2}$	2.158 ± 0.038
4545.19	$8s_{1/2} \to 3p_{3/2}$	
4664.69	$6d_{3/2} \to 3p_{1/2}$	2.154 ± 0.037
4668.47	$6d_{3/2|5/2} \to 3p_{3/2}$	
4747.88	$7s_{1/2} \to 3p_{1/2}$	2.189 ± 0.035
4751.86	$7s_{1/2} \to 3p_{3/2}$	
4978.52	$5d_{3/2} \to 3p_{1/2}$	2.131 ± 0.032
4982.78	$5d_{3/2|5/2} \to 3p_{3/2}$	
5148.66	$6s_{1/2} \to 3p_{1/2}$	2.175 ± 0.030
5153.31	$6s_{1/2} \to 3p_{3/2}$	
5682.54	$4d_{3/2} \to 3p_{1/2}$	2.173 ± 0.024
5688.20	$4d_{3/2|5/2} \to 3p_{3/2}$	
5889.95	$3p_{3/2} \to 3s_{1/2}$	2.151 ± 0.022
5895.97	$3p_{1/2} \to 3s_{1/2}$	
6154.18	$5s_{1/2} \to 3p_{1/2}$	2.150 ± 0.021
6160.75	$5s_{1/2} \to 3p_{3/2}$	

The splitting of the doublets could be written as $\Delta E = \frac{\Delta \lambda}{\lambda^2} \cdot hc$; therefore, as in the hydrogen/deuterium case, the energy splitting uncertainties depend largely on the differences between two measurements of similar wavelengths. As a result, the uncertainties in wavelength difference is reduced as compared to the general case in a similar way as the hydrogen spectra, resulting in the wavelength shift having an uncertainty of 0.06 Å.

From the data, we see that most of the transitions seen are to the $3p$ orbital, with noticeable splitting due to different angular momenta. Transitions from the $4d - 8d$ and $5s - 9s$ to the $3p$ orbital were seen. In addition, transitions from the $4p$ and $3p$ orbital to the $3s$ level were also seen. This is consistent with known selection rules, which dictate that $\Delta J = 0, \pm 1$ and $\Delta l = \pm 1$. [7]

The splitting of the $3p$ level is remarkably consistent across all transitions observed. All of the measurements agree with their average within a 2σ bound, and they lead to a final value of the splitting of

$$\Delta E_{3p_{3/2}, 3p_{1/2}} = (2.155 \pm 0.010)\,\mathrm{meV}.$$

[8] gives the sodium doublet splitting as $1.73 \times 10^3\,\mathrm{m}^{-1}$, corresponding to $2.15\,\mathrm{meV}$, which the computed value is in agreement with.

The energies of orbitals with the same principal quantum number are markedly different, in contrast to Hydrogen, where the orbitals are of nearly the same energy. The orbital splitting is supposedly semi-empirically proportional to $\frac{1}{n^3 \ell(\ell+1)}$. In actuality, the ratio of the 3p-splitting to the 4p-splitting energies is found to be 3.01 ± 0.31, which is not in agreement with the $\frac{4^3}{3^3} \approx 2.37$ predicted by the semi-empirical rule. However, the rule itself is only an approximation, and the computed energy-splitting ratio is still relatively close to that predicted by the rule.

V. CONCLUSION

In this experiment, we used a high-precision monochromator to probe the emission lines of hydrogen, deuterium, and sodium. From the spectral lines, we calculate the Rydberg constant to be $R_H = (1.096764 \pm 0.000013_{stat} \pm 0.000070_{sys}) \cdot 10^7 \mathrm{m}^{-1}$, the hydrogen-deuterium mass ratio to be 0.495 ± 0.012, and the splitting of the 3p-orbitals of sodium to be $(2.155 \pm 0.010)\,\mathrm{meV}$. These values are all within 1σ of the accepted value.

[1] MIT Department of Physics, "Optical spectroscopy of hydrogenic atoms," http://web.mit.edu/8.13/www/JLExperiments/JLExp17.pdf.

[2] "NIST Atomic Spectra Database," https://physics.nist.gov/PhysRefData/ASD/lines_form.html.

[3] "Optical constants of air," https://refractiveindex.info/?shelf=other&book=air&page=Ciddor.

[4] "Refractive index of air depending on temperature," https://physics.stackexchange.com/questions/6872/refractive-index-of-air-depending-on-temperature.

[5] "Fine structure," https://en.wikipedia.org/wiki/Fine_structure.

[6] "CODATA Value: deuteron-proton mass ratio - NIST," https://physics.nist.gov/cgi-bin/cuu/Value?mdsmp.

[7] "Radiative transitions," https://web.archive.org/web/20050426215707/http://www.shef.ac.uk/physics/teaching/phy332/atomic_physics3.pdf.

[8] A. Melissinos and J. Napolitano, "Experiments in modern physics," (Academic Press, 2003) 2nd ed.